

Inelastic electron tunneling spectroscopy for molecular detection

Yasaman Hamidi Zadeh and Zahid A. K. Durrani

Citation: *Journal of Vacuum Science & Technology B* **32**, 06F601 (2014); doi: 10.1116/1.4897137

View online: <http://dx.doi.org/10.1116/1.4897137>

View Table of Contents: <http://scitation.aip.org/content/avs/journal/jvstb/32/6?ver=pdfcov>

Published by the AVS: Science & Technology of Materials, Interfaces, and Processing

Articles you may be interested in

[Analysis of rich inelastic electron tunneling spectra: Case study of terthiophene on Au\(111\)](#)

Rev. Sci. Instrum. **84**, 043907 (2013); 10.1063/1.4803008

[Identification of the atomic scale structures of the gold-thiol interfaces of molecular nanowires by inelastic tunneling spectroscopy](#)

J. Chem. Phys. **136**, 014703 (2012); 10.1063/1.3671455

[Tunneling spectroscopy of electron subbands in thin silicon-on-insulator metal-oxide-semiconductor field-effect transistors](#)


Appl. Phys. Lett. **96**, 112102 (2010); 10.1063/1.3360224

[Study on the interface thermal stability of metal-oxide-semiconductor structures by inelastic electron tunneling spectroscopy](#)





Appl. Phys. Lett. **88**, 262909 (2006); 10.1063/1.2219140

[Aluminum, oxide, and silicon phonons by inelastic electron tunneling spectroscopy on metal-oxide-semiconductor tunnel junctions: Accurate determination and effect of electrical stress](#)

J. Appl. Phys. **96**, 5042 (2004); 10.1063/1.1775299



Instruments for Advanced Science

 <p>Gas Analysis</p> <ul style="list-style-type: none">dynamic measurement of reaction gas streamscatalysis and thermal analysismolecular beam studiesdissolved species probesfermentation, environmental and ecological studies	 <p>Surface Science</p> <ul style="list-style-type: none">UHV TPDSIMSend point detection in ion beam etchelemental imaging - surface mapping	 <p>Plasma Diagnostics</p> <ul style="list-style-type: none">plasma source characterizationetch and deposition process reactionkinetic studiesanalysis of neutral and radical species	 <p>Vacuum Analysis</p> <ul style="list-style-type: none">partial pressure measurement and control of process gasesreactive sputter process controlvacuum diagnosticsvacuum coating process monitoring
--	---	---	---

Contact Hiden Analytical for further details:
W www.HidenAnalytical.com
E info@hiden.co.uk
CLICK TO VIEW our product catalogue

Inelastic electron tunneling spectroscopy for molecular detection

Yasaman Hamidi Zadeh^{a)} and Zahid A. K. Durrani

Optical and Semiconductor Device Group, Department of Electrical and Electronic Engineering,
 Imperial College London, South Kensington, London SW7 2AZ, United Kingdom

(Received 24 June 2014; accepted 23 September 2014; published 2 October 2014)

Inelastic electron tunneling spectroscopy (IETS) [R. C. Jaklevic and J. Lambe, *Phys. Rev. Lett.* **17**, 1139 (1966); R. G. Keil *et al.*, *Appl. Spectrosc.* **30**, 1 (1976); K. W. Hipps and U. Mazur, *J. Phys. Chem.* **97**, 7803 (1993); U. Mazur *et al.*, *Anal. Chem.* **64**, 1845 (1992); P. K. Hansma, *Tunneling Spectroscopy* (Plenum, New York, 1982)] measurements are performed on Si nanowire (NW)/SiO₂/Al NW tunnel junctions. The tunnel junction area is $\sim 50 \times 120$ nm and tunneling occurs across a 10 nm thick SiO₂ layer. IETS measurements are performed at 300 K for ammonium hydroxide (NH₄OH), acetic acid (CH₃COOH), and propionic acid (C₃H₆O₂) molecules. The I - V , dI/dV - V , and d^2I/dV^2 - V characteristics of the tunnel junction are measured before and after the adsorption of molecules on the junction using vapor treatment or immersion. Peaks can be observed in the d^2I/dV^2 - V characteristics in all the cases following molecules adsorption. These peaks may be attributed to vibrational modes of N-H and C-H bonds. © 2014 American Vacuum Society. [<http://dx.doi.org/10.1116/1.4897137>]

I. INTRODUCTION

Inelastic electron tunneling spectroscopy (IETS) provides a means to characterize the phonon spectrum of molecules by measuring phonon-assisted tunneling current through a potential barrier impregnated with the molecules of interest.¹⁻⁵ Traditionally, this technique has used metal/insulator/metal (MIM) junctions and molecules are adsorbed on to the insulator during junction fabrication. At low applied voltage V , tunneling through the barrier is elastic. However, inelastic tunneling caused by electron interaction with vibrational states in the adsorbed molecules creates additional conduction channels, with a change in energy $\hbar\omega$. These lead to peaks in the d^2I/dV^2 vs V characteristics for each additional channel, providing a spectrum of the molecular vibrational modes (Fig. 1). As energy separations in the vibrational spectrum are relatively small compared to the electronic spectrum, in many cases the full vibrational spectrum can be measured only at low temperature⁴ < 30 K. However, it may be possible to measure part of the spectrum even at room temperature, raising the possibility of a molecular detector.

IETS may provide a spectroscopic technique with high sensitivity and selectivity⁶ for gas sensing.⁷ However, the use of IETS for sensing applications requires molecule adsorption only after device fabrication. Bommisetty *et al.* have measured and contrasted the full IETS characteristics for an NH₃ doped, 20×20 μm Al/Al₂O₃/Pb junction at 4 K, with the corresponding characteristic at 300 K.^{7,8} Two large peaks corresponding to Al-O and NH₃ phonons persist even at 300 K, providing a means to identify the underlying molecules bonds.⁸ More recently, the IETS molecular spectra have been measured using scanning tunneling microscopy (STM-IETS).⁹⁻¹¹ This allows the characterization of single molecules with simultaneous imaging of the surface with atomic resolution,⁹ e.g., STM

measurements have been performed on single acetylene molecules.⁹ Single molecule spectra have also been measured using micrometer scale metal/molecule/metal junction measurements of alkyl and π -conjugated molecules,¹² and nanoscale alkanedithiol monolayers.¹³

In this paper, IETS measurements are presented for nanoscale semiconductor/insulator/metal tunnel junctions [Si nanowire (NW)/SiO₂/Al NW] (Fig. 2). Our use of a Si NW provides a means to define a more robust tunnel junction with the potential for gate control. The molecules of interest are adsorbed on to the insulator after device fabrication. At low applied voltage, the tunneling process is similar to a MIM device. However, as the applied voltage increases, the electrical characteristics are affected by the Schottky barrier formed at the Si NW surface. With a reverse biased Schottky barrier, IETS peaks may be measured at reduced current, with less likely hood of damaging the tunnel junctions.

IETS measurements are performed on well-characterized molecules such as NH₄OH, CH₃COOH, and C₃H₆O₂ at room temperature. The I - V , dI/dV - V , and d^2I/dV^2 - V characteristics of the tunnel junction are measured before and after the adsorption of the ammonium hydroxide (NH₄OH), acetic acid (CH₃COOH), and propionic acid (C₃H₆O₂) molecules using vapor treatment for NH₄OH molecules and immersion for CH₃COOH and C₃H₆O₂ molecules.

II. FABRICATION

Nanoscale (Si NW/SiO₂/Al NW) tunnel junctions were fabricated using electron beam lithography (EBL). Here, the Si NW (Refs. 14-16) was fabricated in heavily doped n-type silicon-on-insulator (SOI) material (doping density $\sim 10^{19}$ - 10^{20} /cm³). Spin-on-doping was used to dope the top Si of the SOI material. Following this, a nanowire pattern was written using EBL in PMMA resist with a molecular weight of 950 000, diluted 2% in Anisole. A 40 nm thick Al

^{a)}Electronic mail: y.hamidi-zadeh10@imperial.ac.uk

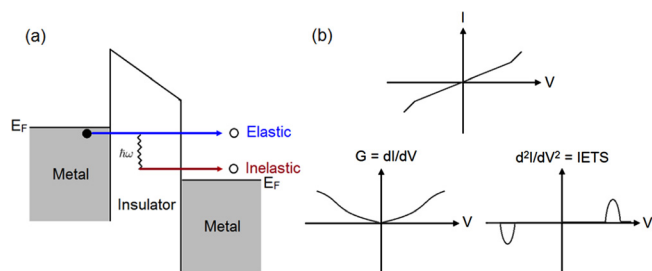


FIG. 1. (Color online) Schematic diagrams of (a) inelastic tunneling and (b) IETS signals (The I - V characteristics, conductance $G = dI/dV$ - V and IETS peaks d^2I/dV^2 - V) for a metal/insulator/metal tunnel junction device.

layer was then evaporated and lift-off used to create a ~ 50 nm wide Al NW. This created a hard mask for reactive ion etching (RIE) of the top Si layer. SF_6 was used as the RIE gas at 100mTorr for 40 s, at RF power of 100 W and an etch depth of 200 nm was obtained. The Al mask was then removed using wet etching for 30 s. Here, the wet-etch contained mixtures of 1%–5% HNO_3 for Al oxidation, 65%–75% H_3PO_4 to dissolve the Al_2O_3 , 5%–10% CH_3COOH for wetting and buffering and H_2O dilution. Si NWs with lengths $\sim 1 \mu\text{m}$ and widths down to ~ 50 nm were fabricated by this process. The NWs were then thermally oxidized at 1000°C to create a SiO_2 surface layer ~ 10 nm thick. A second EBL stage was then used to define a 40 nm thick and ~ 120 nm wide Al NW such that it crossed the Si NW, forming the nanoscale Si NW/ SiO_2 /Al NW tunnel junction. Figure 3 shows scanning electron micrograph (SEM) of a complete device.

The reduction in device dimension to the nanoscale is expected to increase the sensitivity of the device to molecules adsorbed on the tunnel junction. Various mechanisms are possible for adsorption of molecules on the tunnel junction: The top Al layer is only ~ 40 nm thick and can be porous.^{17–20} Molecules can then diffuse through the pores in a manner similar to previous work on large area IETS structures with thin Al contacts (~ 50 nm).¹⁹ In particular, molecules in the presence of water vapor can penetrate the top metal of the completed tunnel junction more easily.^{17–20} A second possible mechanism, involves the deposition and diffusion of molecules from the exposed SiO_2 surface at the side edges of the tunnel junction. Furthermore, the use of SOI material raises the possibility of back gate control of the

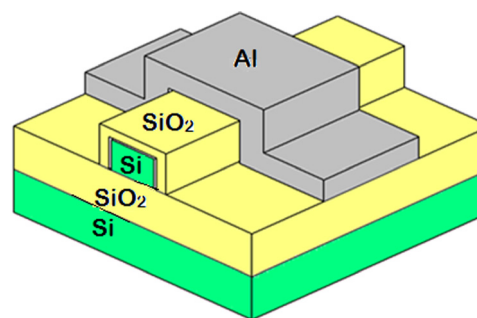


FIG. 2. (Color online) Schematic diagram of a crossed Si NW/ SiO_2 /Al NW tunnel junction.

NW carrier concentration, and hence of the IETS characteristics.

III. MEASUREMENT

IETS measurements were performed at room temperature by using an Agilent 4155B parameter analyzer to obtain four terminal I - V characteristics (1000 measurement points). The dI/dV - V and d^2I/dV^2 - V characteristics were then calculated from the data. The noise floor in our I - V measurement was ~ 10 pA, allowing direct extraction of d^2I/dV^2 - V curves. Tunneling spectra were measured for NH_4OH , CH_3COOH , and $\text{C}_3\text{H}_6\text{O}_2$. Here, NH_4OH was deposited on the device by vapor treatment and CH_3COOH and $\text{C}_3\text{H}_6\text{O}_2$ by immersion. The four-terminal measurement circuit is shown in Fig. 4(a). Current was forced through the tunnel junction using terminals 2 (Al NW) and 1 (Si NW) and the voltage was measured between terminals 4 (Al NW) and 3 (Si NW).

A. Ammonium hydroxide (NH_4OH)

Electrical characteristics of a “clean” tunnel junction were measured first at 300 K. The dI/dV - V and d^2I/dV^2 - V were then calculated numerically. As the device could not be immersed directly in ammonium hydroxide, vapor treatment is used to deposit NH_3 vapor molecules on the device. Here, the device was left in a petri dish in an ammonium hydroxide atmosphere for 2 h. Measurements were then repeated and compared to those from the clean device [Figs. 4(b)–4(d)]. It is possible to wash the device in acetone/isopropyl alcohol

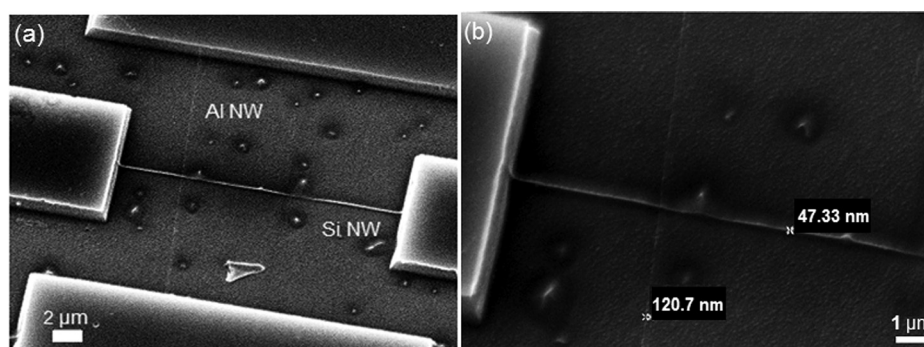


FIG. 3. (a) Magnified SEM image of Si NW/ SiO_2 /Al NW tunnel junction and (b) SEM image of Si NW/ SiO_2 /Al NW tunnel junction widths.

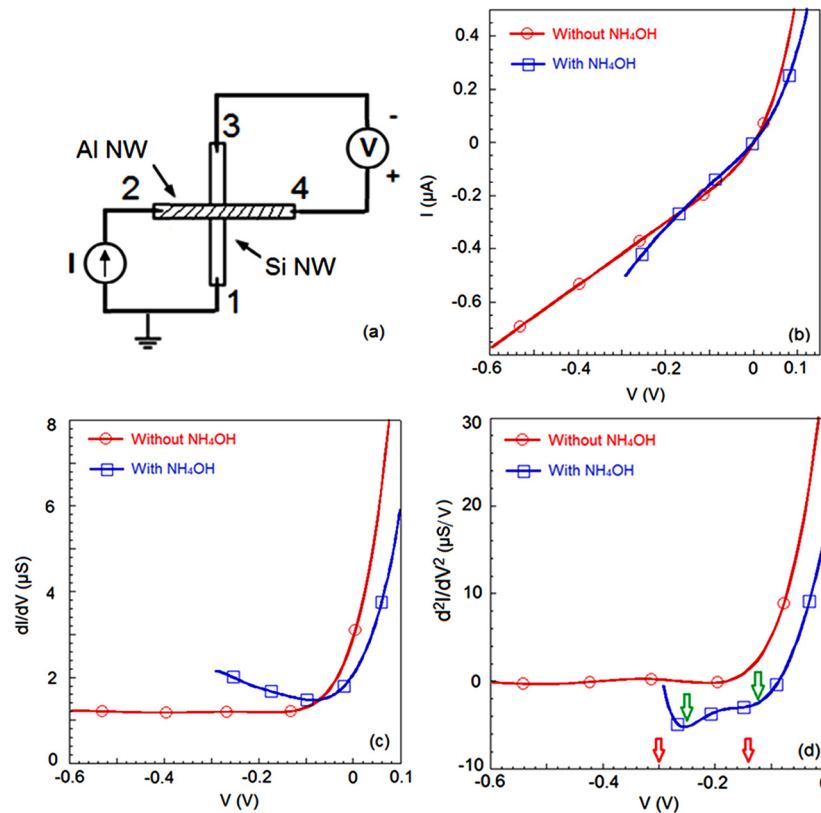


FIG. 4. (Color online) IET spectrum of NH_4OH on a Si NW/ SiO_2 /Al NW tunnel junction at 300 K (1000 measurement points, rectangles and circles used as marker to indicate different curves): (a) four-terminal measurement circuit, (b) the I - V characteristics of the tunnel junction before and after adsorption of NH_4OH molecules, (c) the dI/dV - V characteristics, and (d) the d^2I/dV^2 - V characteristics of the device.

and recover the original clean measurement. This is in contrast to early IETS measurements where molecules were introduced during the tunnel junction fabrication.¹⁻⁴

Figure 4(b) illustrates the I - V characteristics of the tunnel junction before and after adsorption of NH_4OH molecules. Figure 4(c) displays the dI/dV - V characteristics, and Fig. 4(d) shows the d^2I/dV^2 - V characteristics of the device. The I - V characteristics [Fig. 4(b)] are diodelike, due to the presence of a Schottky barrier at the Si NW/ SiO_2 interface. As we measure the data using a four-terminal measurement, this implies that the Schottky barrier must lie along the current path, i.e., at the interface and is not remote from the junction elsewhere in the Si NW (Fig. 5). The device current reduces slightly following NH_4OH treatment. In the d^2I/dV^2 - V characteristics [Fig. 4(d)], peaks are observed at ~ -0.12 and -0.25 V (upper arrows). These may be attributed to the first and second excitation modes of an N-H bond at room temperature.

The lower arrows at ~ -0.15 and -0.3 V indicate previously reported excitation modes of N-H bonds in a MIM Al/ Al_2O_3 /Pb device at 4.2 K.²¹ The peaks in our data are shifted slightly relative to previous data. However, the peaks' separation remains the same at ~ -0.15 V.

B. Acetic acid (CH_3COOH)

The IETS characteristics of a tunnel junction with acetic acid adsorption are shown in Fig. 6. Figures 6(a)-6(c)

shows the I - V , dI/dV - V , and d^2I/dV^2 - V characteristics, respectively, for both the clean device, and the device with acetic acid adsorption. Acetic acid was adsorbed on

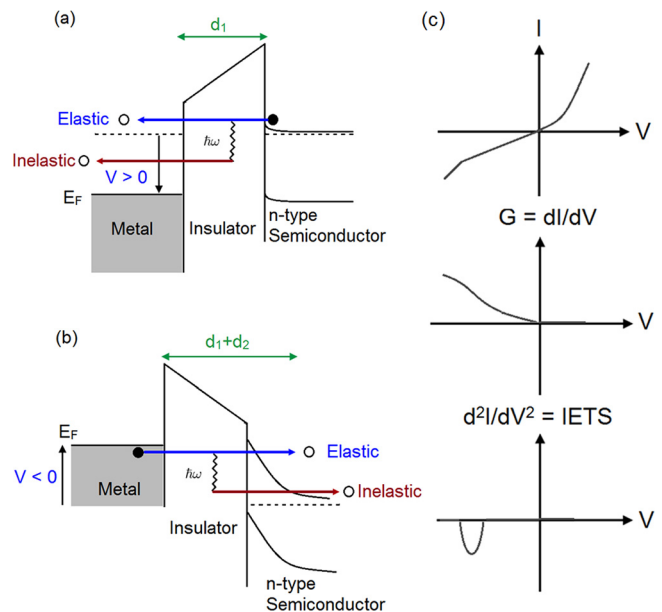


FIG. 5. (Color online) (a) Inelastic tunneling forward bias, (b) inelastic tunneling reverse bias, and (c) IETS signals (The I - V characteristics, conductance $G = dI/dV$ - V and IETS peaks d^2I/dV^2 - V) for semiconductor/insulator/metal tunnel junction.

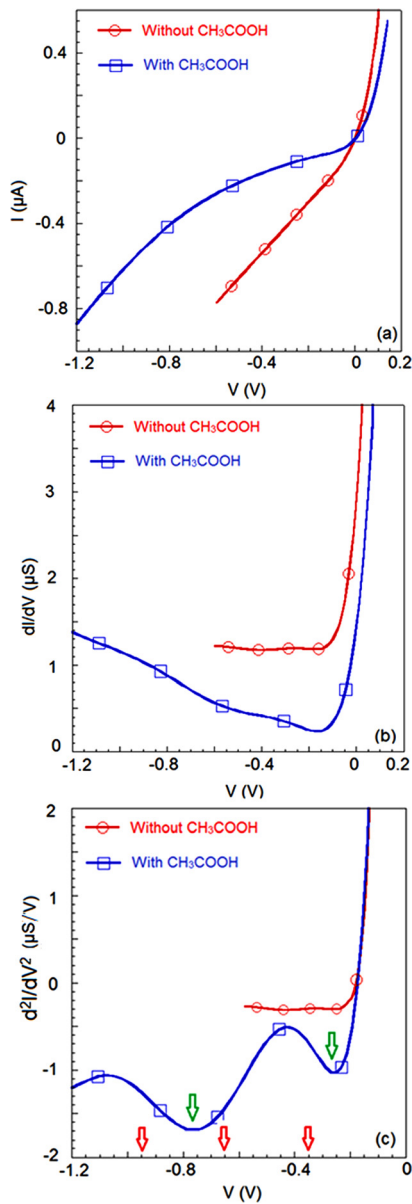


FIG. 6. (Color online) IET spectrum of CH_3COOH on a Si NW/ SiO_2 /Al NW tunnel junction at 300 K: (a) The I - V characteristics, for both the clean device, and the device with acetic acid adsorption. (b) The dI/dV - V characteristics, for both the clean device, and the device with acetic acid adsorption. (c) The d^2I/dV^2 - V characteristics, for both the clean device, and the device with acetic acid adsorption. (Note: 1000 measurement points, rectangles and circles used as marker to indicate different curves.)

the clean device by immersion at room temperature for 5 min.

In a manner similar to the measurements of Fig. 4(b), the I - V characteristics are diodelike, both before and after immersion, and the device current reduces following immersion. The dI/dV - V characteristics of the device [Fig. 6(b)] show a reduction in conductance, and nonlinearities that correspond to the peaks in the d^2I/dV^2 - V characteristics. In Fig. 6(c), the upper arrows indicate the measured peaks at ~ -0.25 and -0.75 V, which may be attributed to the first and third excitation modes of a C-H bond at room temperature. The lower arrows illustrate the previously reported excitation modes of C-H at ~ -0.36 , -0.65 , and -0.95 V in a

MIM device at 4.2 K.²² The peaks' separation in our measured data is ~ -0.5 V, which corresponds well to the separation between the first and third excitation modes of C-H bonds.

C. Propionic acid ($\text{C}_3\text{H}_6\text{O}_2$)

The IETS characteristics of a tunnel junction with $\text{C}_3\text{H}_6\text{O}_2$ adsorption are shown in Fig. 7. Figures 7(a)-7(c) shows the I - V , dI/dV - V , and d^2I/dV^2 - V characteristics, respectively, for both the clean device, and the device with

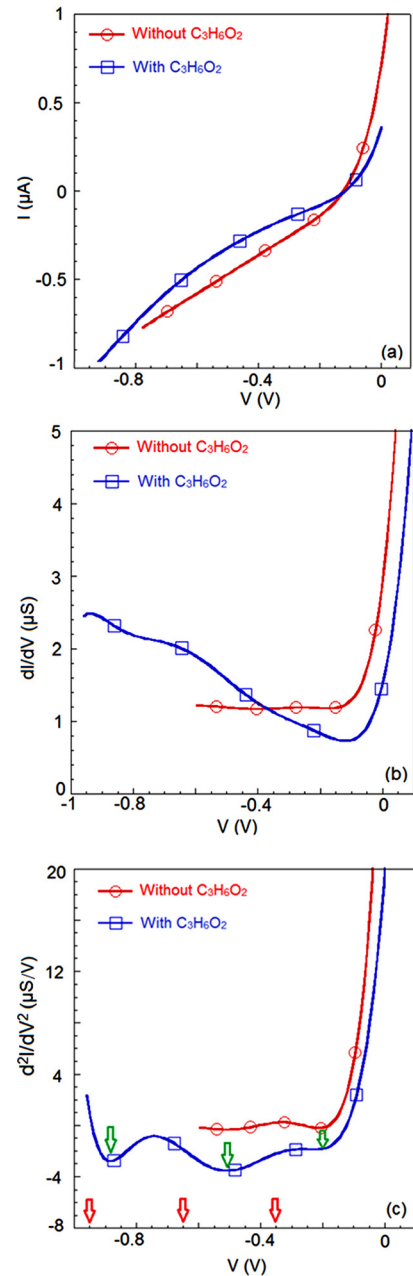


FIG. 7. (Color online) IET spectrum of $\text{C}_3\text{H}_6\text{O}_2$ on a Si NW/ SiO_2 /Al NW tunnel junction at 300 K: (a) The I - V characteristics, for both the clean device, and the device with propionic acid adsorption. (b) The dI/dV - V characteristics, for both the clean device, and the device with propionic acid adsorption. (c) The d^2I/dV^2 - V characteristics, for both the clean device, and the device with acetic propionic adsorption. (Note: 1000 measurement points, rectangles and circles used as marker to indicate different curves.)

propionic acid adsorption. Propionic acid was adsorbed on the clean device by immersion at room temperature for 5 min.

In a manner similar to the measurements of Figs. 4(b) and 6(a), the I - V characteristics are diodelike, both before and after immersion, and the device current reduces following immersion. Figure 7(b), the dI/dV - V characteristics of the device, show a reduction in conductance and nonlinearities, which correspond to the peaks in the d^2I/dV^2 - V characteristics. In Fig. 7(c), the upper arrows illustrate measured peaks at ~ -0.2 , -0.5 , and -0.85 V, which may be attributed to the first, second, and third excitation modes of a C-H bond at room temperature.

The lower arrows illustrate the previously reported excitation modes of C-H at ~ -0.36 , -0.65 , and -0.95 V in a MIM device at 4.2 K.²² The peaks' separation in our measured data is ~ -0.3 V, which corresponds well to the separation between the first and second and also between the second and third excitation modes of C-H bond.

IV. SUMMARY

IETS measurements are performed on Si NW/SiO₂/Al NW tunnel junctions at 300 K for NH₄OH, CH₃COOH, and C₃H₆O₂ molecules. The tunnel junction area is $\sim 50 \times 120$ nm and tunneling occurs across the 10 nm thick SiO₂ layer. The I - V , dI/dV - V , and d^2I/dV^2 - V characteristics of the tunnel junction are measured before and after the adsorption of the NH₄OH, CH₃COOH, and C₃H₆O₂ molecules using vapor treatment or immersion. Peaks can be observed in the d^2I/dV^2 - V characteristics in all the cases following molecules adsorption. These peaks may be attributed

to the vibrational modes of N-H and C-H bonds. The peak separations are similar to previous reported work on micrometer scale MIM tunnel junction at low temperature.

- ¹R. C. Jaklevic and J. Lambe, *Phys. Rev. Lett.* **17**, 1139 (1966).
- ²R. G. Keil, T. P. Graham, and K. P. Roenker, *Appl. Spectrosc.* **30**, 1 (1976).
- ³K. W. Hipps and U. Mazur, *J. Phys. Chem.* **97**, 7803 (1993).
- ⁴U. Mazur, X. D. Wang, and K. W. Hipps, *Anal. Chem.* **64**, 1845 (1992).
- ⁵P. K. Hansma, *Tunneling Spectroscopy* (Plenum, New York, 1982).
- ⁶U. Mazur and K. W. Hipps, "Inelastic electron tunnelling spectroscopy," in *Handbook of Vibrational Spectroscopy*, edited by J. Chalmers and P. Griffiths (John Wiley and Sons Ltd, Chichester, 2002).
- ⁷V. BommiSETTY, S. Bhandari, R. L. Karmacharya, D. A. Rislov, R. D. Mileham, and D. W. Galipeau, *IEEE Sens. J.* **8**, 983 (2008).
- ⁸D. G. Walmsley and J. L. Tomlin, *Prog. Surf. Sci.* **18**, 247 (1985).
- ⁹B. C. Stipe, M. A. Rezaci, and W. Ho, *Science* **280**, 1732 (1998).
- ¹⁰Y. Sainoo, Y. Kim, T. Komeda, and M. Kawai, *J. Chem. Phys.* **120**, 7249 (2004).
- ¹¹N. Okabayashi, Y. Konda, and T. Komeda, *Phys. Rev. Lett.* **100**, 217801 (2008).
- ¹²J. G. Kushmerick, J. Lazorik, C. H. Patterson, R. Shashidhar, D. S. Seferos, and G. C. Bazan, *Nano Lett.* **4**, 639 (2004).
- ¹³W. Wang, T. Lee, I. Kretzschmar, and M. A. Reed, *Nano Lett.* **4**, 643 (2004).
- ¹⁴A. Agarwal, K. Buddharaju, I. K. Lao, N. Singh, N. Balasubramanian, and D. L. Kwong, *Sens. Actuators, A* **145**, 207 (2008).
- ¹⁵E. Stern *et al.*, *Nature* **445**, 519 (2007).
- ¹⁶D. Wang, B. A. Sheriff, and J. R. Heath, *Nano Lett.* **6**, 1096 (2006).
- ¹⁷W. J. Nelson, D. G. Walmsley, and J. M. Bell, *Thin Solid Films* **79**, 229 (1981).
- ¹⁸M. Higo, X. Lu, U. Mazur, and K. W. Hipps, *Chem. Lett.* **28**, 679 (1999).
- ¹⁹J. R. Bellingham, C. J. Adkins, and W. A. Phillips, *Thin Solid Films* **198**, 85 (1991).
- ²⁰K. W. Hipps and U. Mazur, *J. Phys. Chem.* **96**, 1160 (1992).
- ²¹G. Herzberg, *Infrared and Raman Spectra* (D. Van Nostrand and Co., New York, 1945).
- ²²J. Lambe and R. C. Jaklevic, *Phys. Rev.* **165**, 821 (1968).